Macromolecules

ARTICLE

pubs.acs.org/Macromolecules

Emulsion Interfacial Synthesis of Asymmetric Janus Particles

Yanhong Wang, Chengliang Zhang,* Chen Tang, Jing Li, Ke Shen, Jiguang Liu, Xiaozhong Qu, Jiaoli Li, Qian Wang, and Zhenzhong Yang*

State Key Laboratory of Polymer Physics and Chemistry, Institute of Chemistry, Chinese Academy of Sciences, Beijing 100190, China

Supporting Information

ABSTRACT: We have proposed a simple method to synthesize asymmetric Janus polymer particles at an emulsion interface. Morphological evolution of the particles with polymerization and their dependence on some key variables reveal that both cross-linking degree of the particles and interfacial tension difference play key roles in achieving the asymmetric shapes. By selective growth of functional materials onto the desired sides, composition and microstructure of the Janus particles can be controlled. The representative PS/PAM Janus particles are amphiphilic and can be used as solid surfactants to stabilize emulsions, which preferentially orientate at the interface.

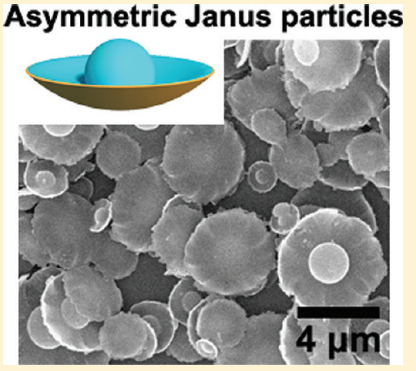

1. INTRODUCTION

Janus particles have two different compositions and properties compartmentalized onto the same surface.[1] They have gained increasing interests due to their unique performances thus promising applications.[2] There are many pursuing applications such as building blocks of complex superstructures,[3] particle surfactants,[4] optical nanoprobes,[5] *stimuli-response*,[6] electrical display,[7] and self-propulsion nanomotor.[8] Many methods have been proposed to synthesize Janus particles, including toposelective modification,[9] surface nucleation,[10] self-assembly of block polymers,[11] microfluidic technique,[12] space-confined assembly,[13] electro-spinning,[14] controlled phase separation,[15] and Pickering emulsion interfacial synthesis.[16] It is significant to control asymmetric shape of Janus particles due to superior performances over the symmetric counterparts. For example, from the asymmetric dumbbell Janus particles, an interesting chiral helix structure formed under a magnetic field due to their additional spatial restriction.[17] Compared with the spherical Janus particles, asymmetric disk-shaped Janus particles can better stabilize an interface due to restricted rotation and enhanced adsorption energy.[4b] Asymmetric shape can also provide enhanced power to propel Janus nanomotors.[8] Among above synthesis methods, Pickering emulsion interfacial synthesis has been extensively employed to synthesize large amount of Janus particles with chemistry distinctly compartmentalized, especially to give asymmetric Janus particles by a subsequent wet-etching.[16e] Although Pickering emulsion interface synthesis possesses lots of potential to control particles shape, almost all particles for Pickering emulsions are preformed and they are not easily deformable at the interface. Even for polymer particles, asymmetric deformation is rather limited.[18] Moreover, the method cannot provide large scale production of Janus particles. Recently, Okubo et al. have proposed an emulsion method to large-scale synthesize polymer Janus particles with interesting mushroom-like morphology.[19] The method essentially relies on preformation of Janus particles with initiator partially covered surface by solvent evaporation induced phase separation. A subsequent surface-initiated ATRP preferentially gives another polymer onto one side, and meanwhile the shape is transformed from the spherical to nonspherical even to mushroom-like with increasing polymerization degree. Deformation of the Janus particles is limited mainly due to restricted ATRP degree. Moreover, it is not clear if the other side has the initiator even at small amount level since the preformed Janus particles are achieved by polymer phase separation.

Herein, we present a method to synthesize asymmetric Janus particles at emulsion interface as illustrated in Scheme 1. First, an oil/water (O/W) emulsion forms in the presence of surfactant sodium dodecyl sulfate (SDS) by high shear emulsification. The oil phase is composed of paraffin wax (T_m: 22−27 °C), oil soluble monomers such as styrene (St), divinylbenzene (DVB) and initiator 2,2′-azobis (isobutyronitrile) (AIBN). The emulsion is heated to 70 °C to initiate the polymerization. The as-formed polymer becomes insoluble, phase separation occurs forming a polymer ball. The ball will migrate toward the O/W interface and anchors thereby due to Pickering effect.[16a] Upon absorption of SDS only onto the exterior side of the ball exposed to the aqueous phase, a temporal Janus structure onto the polymer ball surface is achieved. It should be noticed that the polymer ball forms in situ and thus is easily

Received: December 24, 2010
Revised: March 8, 2011
Published: April 28, 2011

Scheme 1. Schematic Synthesis of the Asymmetric Janus Polymer Particles at the Interface of Emulsion Droplets[a]

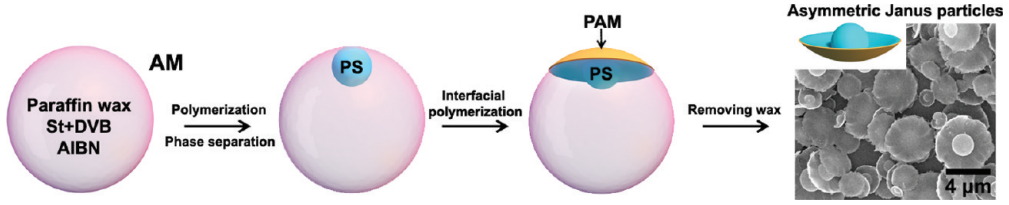

[a] For a more detailed description see the text.

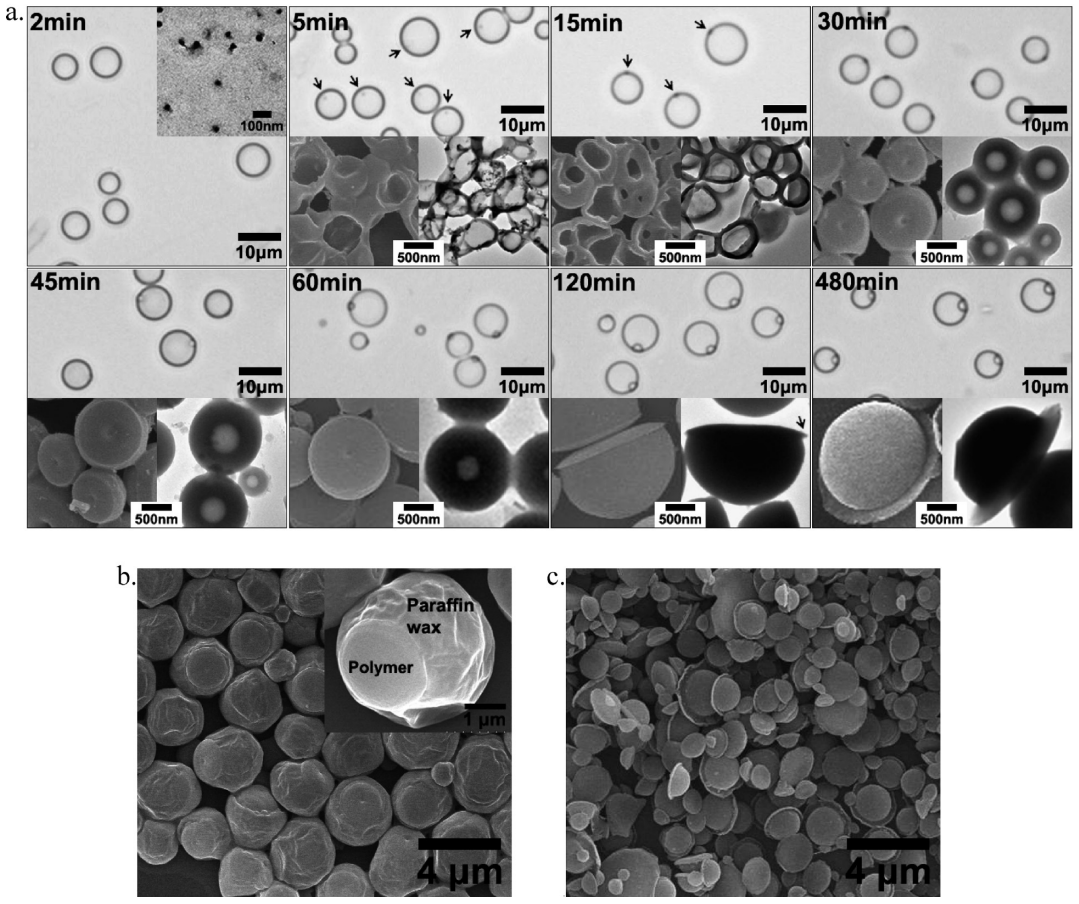

Figure 1. (a) Optical micrographs of the oil droplets and inset SEM and TEM images of the polymer particles synthesized at varied polymerization time after removing oil phase. The recipe was given as in the experimental synthesis section but without AM. SEM images of the polymer particles using the paraffin wax (T_m: 52−54 °C) as oil phase: (b) before and (c) after dissolution of the paraffin wax.

deformable, especially at an early stage of polymerization. At the triple phase contact line, the interfacial tension difference between water/oil and water/polymer will elongate the polymer ball exterior side exposed to the aqueous phase. As a result, an edge forms that evolves progressively to a larger disk with further polymerization of residual monomers enriched there. The polymer ball becomes asymmetric in shape. When water-soluble monomers such as acrylamide (AM) are present in the aqueous phase, residual free radicals at the asymmetric ball will initiate polymerization of AM forming hydrophilic polymer brush onto the exposed exterior side. Chemistry of the two sides becomes different thus achieving permanent Janus performance. After the paraffin wax is dissolved, the corresponding asymmetric for example ball-on-disk structure Janus particles are obtained. It is more flexible to tune the deformation of the Janus particles. Moreover, the two compositions are distinctly compartmentalized onto both sides.

2. EXPERIMENTAL METHODS

2.1. Materials. Monomers styrene (St) and acrylamide (AM), surfactant sodium dodecyl sulfate (SDS), initiator 2,2′-azobis (isobutyronitrile) (AIBN), silica precursor tetraethoxysilane (TEOS), *n*-heptane were purchased from Sinopharm Chemical Reagent Beijing Co. All chemicals are analytical grade. Divinylbenzene (DVB) was purchased from Aldrich. St and DVB were destabilized over Al_2O_3 column and then stored at low temperature. All other reagents were used as received. Two paraffin waxes

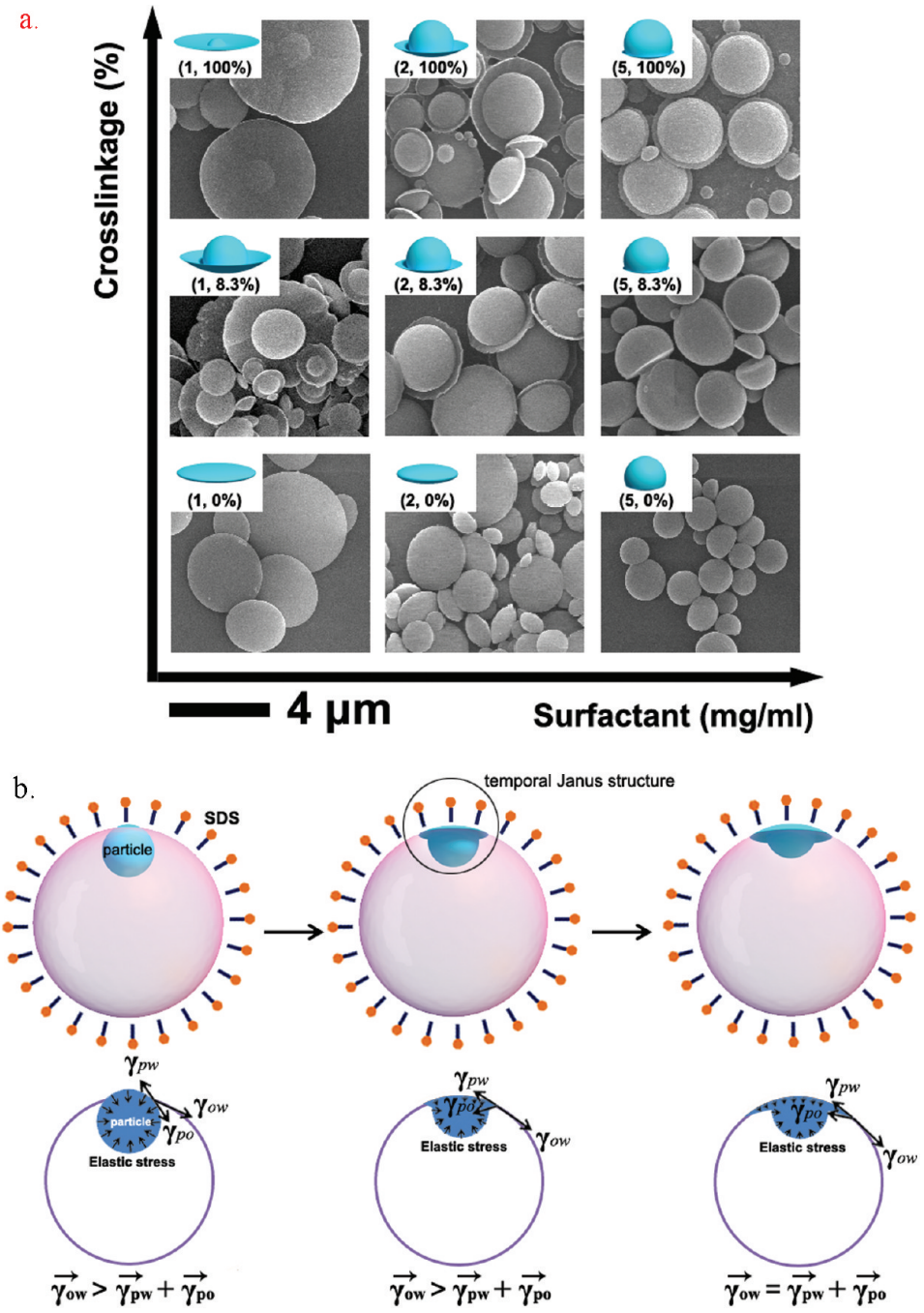

Figure 2. (a) Final morphology of the asymmetric polymer particles dependent on two variables of surfactant (SDS) concentration and cross-linking degree (DVB percentage in the monomer mixture). (b) Schematic analysis of interfacial tensions contribution to the formation of the ball-on-disk structure.

(T_m: 22−27 and 52−54 °C) were purchased from Nan Yang Wax Fine Chemical Plant.

2.2. Synthesis of Asymmetric Janus PS/PAM Particles. An example recipe is given as following. 5.5 g of St, 0.5 g of DVB, 0.12 g of AIBN, 0.2 g of SDS, 10 g of paraffin wax, 84 g of water were emulsified at 70 °C at a stirring speed of 12000 rpm for 2 min. Afterward, the emulsion polymerization was initiated at 70 °C. After 15 min, a solution of 1 g of AM in 5 g of water was added to the emulsion. The polymerization was kept for 7 h. The PS/PAM/paraffin wax particles were obtained after centrifugation at room temperature. After paraffin wax was dissolved by excess ethanol, the Janus PS/PAM asymmetric particles were obtained.

2.3. Synthesis of Janus PS/SiO_2 Composite Particles. A 0.03 g sample of freeze-dried powder of PS/PAM Janus particles was dispersed in 2.5 g of ethanol, 1 g of water, and 0.5 g of aqueous ammonia (28 wt %). Then, 0.003 g of TEOS was dropped into the dispersion. A sol−gel process was carried out under stirring for 24 h at room temperature. After centrifugation and a wash with ethanol, the Janus PS/SiO_2 composite particles were obtained.

2.4. Synthesis of Janus PS/Fe_3O_4 Composite Particles. A 0.1 g sample of freeze-dried powder of the Janus PS/PAM particles was dispersed in 5 g of water. Afterward, 10 g of citric acid capped Fe_3O_4 nanoparticles aqueous dispersion (0.5 wt %) was added under ultrasonic

dx.doi.org/10.1021/ma102945t |*Macromolecules* 2011, 44, 3787–3794

for 10 min. The Janus PS/Fe_3O_4 composite particles were obtained after centrifugation.

2.5. Emulsification Using the Janus PS/PAM Particles. A 0.006 g sample of freeze-dried powder of the PS/PAM Janus particles was dispersed in 2.5 g of water, followed by adding 0.5 g of styrene. After the mixture was emulsified under ultrasonication at room temperature for 10 min, the oil-in-water emulsion formed. Similarly, 0.006 g of the Janus particles was dispersed in 2.5 g of *n*-heptane and 0.5 g of water, and the corresponding water-in-oil emulsion formed.

2.6. Characterization. Ethanol was used as dispersion agent to avoid aggregation between the Janus particles. Morphology of the particles was characterized using transmission electron microscopy (JEOL 1011 at 100 kV) and scanning electron microscopy (Hitachi S-4300 and S-4800 at 15 kV) equipped with an energy dispersive X-ray (EDX) analyzer. The samples for SEM observation were prepared by vacuum sputtering with Pt after being ambient dried. The samples for TEM observation were prepared by spreading very dilute dispersions in ethanol onto carbon-coated copper grids. FT-IR spectroscopy was performed using a Bruker EQUINOX 55 spectrometer with the sample/KBr pressed pellets.

Table 1. Surface Tension (γ_w) of SDS Solution, Contact Angle (θ) of SDS Solution on PS Film, and Interfacial Tension (γ_{ow}) of SDS Solution/Paraffin Wax (T_m: 22−27 °C) Depending on SDS Concentration[a]

SDS concentration (mg/mL)	1	2	5
γ_w (mN/m)	48	39	37
θ (deg)	44.5	27.8	20.4
γ_{ow} (mN/m)	5.635	2.838	1.944

[a] All measurements were performed at 30 °C. γ_w was measured by DCAT 11EC (Dataphysics). Contact angle was measured on a Krüss DSA100 system with a SDS solution droplet of 5 μL on PS film (the cross-linkage is 8.3% DVB). γ_{ow} was measured by interfacial tensiometer TX500C (Bowing Industry Co.). (1) In the case of decreasing in SDS concentration from 5 to 2 mg/mL: $\Delta\gamma_{pw} = (\gamma_p - \gamma_w \cos\theta)_{SDS=2} - (\gamma_p - \gamma_w \cos\theta)_{SDS=5}$, since $\gamma_{p\ SDS=2} = \gamma_{p\ SDS=5}$, $\Delta\gamma_{pw} = (\gamma_w\cos\theta)_{SDS=5} - (\gamma_w\cos\theta)_{SDS=2} = 37 \times \cos 20.4° - 39 \times \cos 27.8° = 0.180$ mN/m, $\Delta\gamma_{ow} = \gamma_{ow\ SDS=2} - \gamma_{ow\ SDS=5} = 2.838 - 1.944 = 0.894$ mN/m. (2) In the case of decreasing in SDS concentration from 2 to 1 mg/mL: $\Delta\gamma_{pw} = (\gamma_w\cos\theta)_{SDS=2} - (\gamma_w\cos\theta)_{SDS=1} = 39 \times \cos 27.8° - 48 \times \cos 44.5° = 0.263$ mN/m, $\Delta\gamma_{ow} = \gamma_{ow\ SDS=1} - \gamma_{ow\ SDS=2} = 5.635 - 2.838 = 2.797$ mN/m.

3. RESULTS AND DISCUSSION

In order to elucidate formation of the asymmetric shapes, structural evolution of the emulsion droplets and the polymer particles with polymerization has been continuously monitored under optical microscope (Figure 1a,b). In order to simplify the observation, no AM is introduced in the aqueous phase. At a very early stage of polymerization (2 min), individual smaller polymer clusters form by polymerization induced phase separation and are dispersed inside the oil phase, which cannot be observed by optical micrograph but TEM image after dissolution of the oil phase. Along polymerization (5 min), these polymer clusters coalesce into one larger sphere, which can be distinctly observed under optical micrograph as indicated by the arrows. After removal of the oil phase, polymer hollow spheres are obtained, indicating that the polymer spheres are highly swollen with monomers. The spheres are eccentric in the oil phase but not anchor at the O/W interface. TEM measurement indicates the PS spheres are about 600 nm in diameter. With further polymerization (15 min), the spheres are less changed in size but anchored at the O/W interface possibly due to the Pickering effect.[16a] SEM image indicates that one side of the spheres becomes flatter. With further polymerization (15−60 min), the spheres become larger; meanwhile, the shell becomes thicker and the cavity smaller. With prolonged polymerization times (120 min), the hollow spheres become solid; meanwhile, an edge appears. At this stage, the polymer domain is cross-linked sufficiently above a certain degree, direct diffusion of residual St/DVB monomers from the paraffin oil droplet into the polymer domain

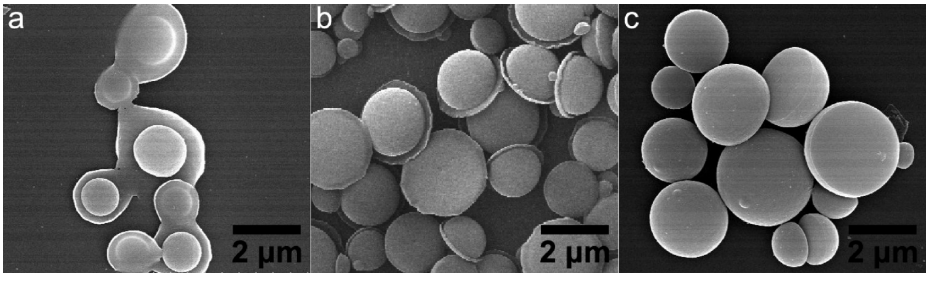

Figure 3. Morphology of three representative polymer particles synthesized at different fraction of the monomers in the oil phase: (a) 23.1 wt %; (b) 37.5 wt %; (c) 54.5 wt %. The oil/water ratio remained constant, and the St/DVB ratio was kept at 11:1.

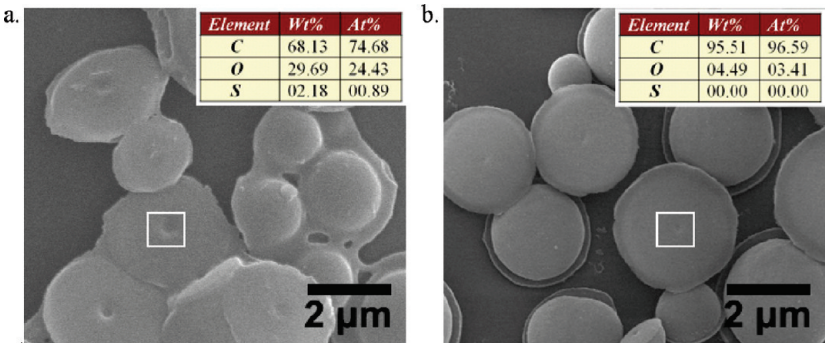

Figure 4. EDX results of the temporal Janus polymer particles after different cycles of washing with ethanol (a) one time and (b) five times. The data show that the S element (corresponding to SDS) is present on the flattened side after washing for one time, but no S element can be detected after washing five times.

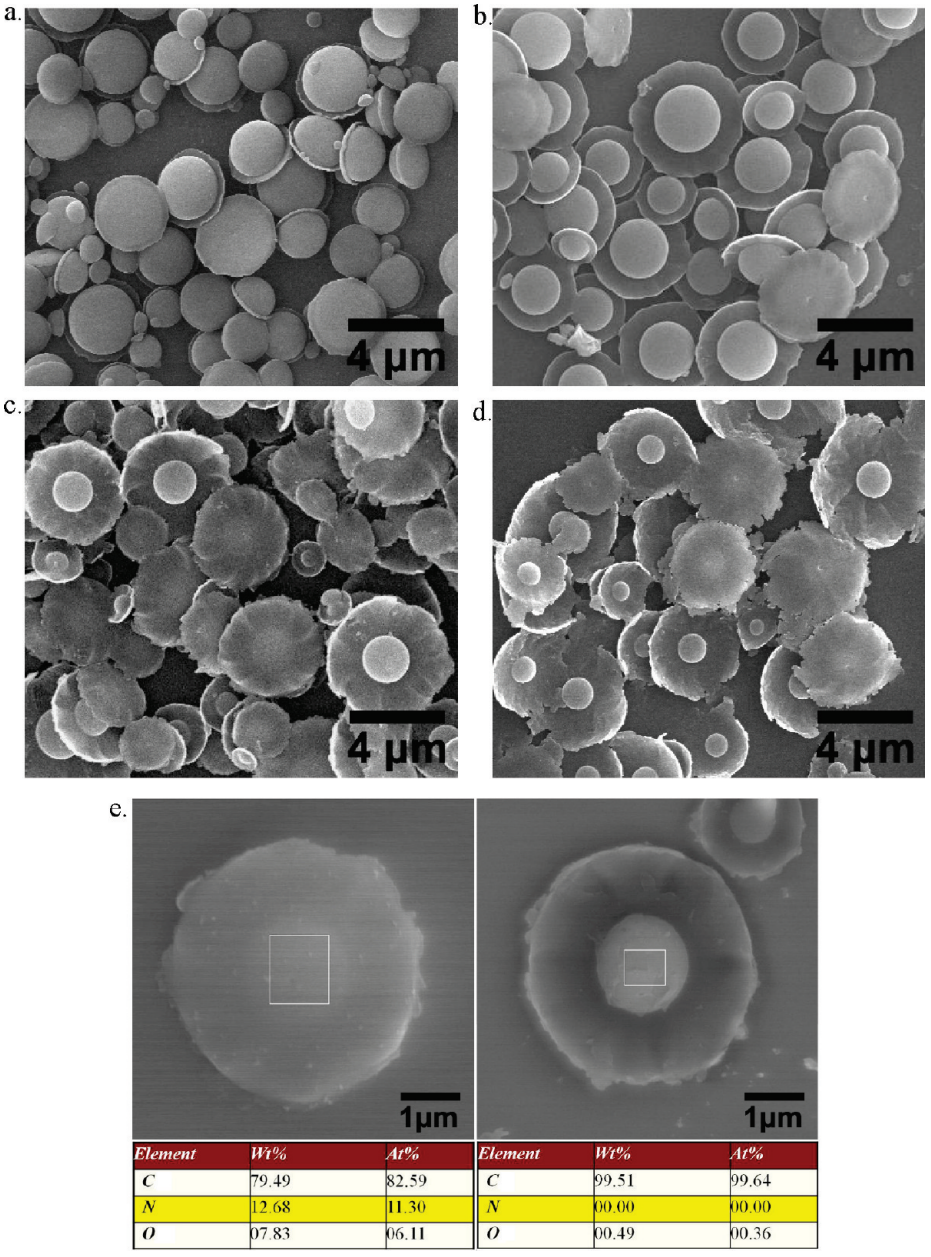

Element	Wt%	At%	Element	Wt%	At%
C	79.49	82.59	C	99.51	99.64
N	12.68	11.30	N	00.00	00.00
O	07.83	06.11	O	00.49	00.36

Figure 5. Morphology of the asymmetric Janus particles with increasing AM content (g): (a) 0; (b) 0.2; (c) 1.0; (d) 2.0. (e) EDX results of both sides of the ball-on-disk asymmetric Janus polymer particles as shown in part c: (left) the disk side; (right) the ball side. The recipe was given in the experimental synthesis section.

through the polymer/paraffin oil interface becomes difficult. Instead, St/DVB monomers can easily diffuse along the paraffin oil droplet/SDS(/water) interface to the interface between polymer and SDS(/water) because of the polymerization driving force inside the polymer domain. Again, the St/DVB monomers accumulated between polymer and SDS(/water) will be difficult to diffuse inside the polymer domain. Instead, the monomers will tend to favorably wet the polymer surface along the triple phase contact line. Subsequent polymerization of the monomers gives "straw hat" thus the "ball-on-disk" nano-object. Edge of the disk is further grown and evolves to disk shape, while the whole particle size keeps less changed with polymerization time (480 min). In order to clarify that the edge (or disk) forms at the exterior side exposed to the aqueous phase, another paraffin wax with high melt temperature (T_m: 52−54 °C) is used instead. When the system is cooled down to room temperature, structure of the oil droplets is fixed. The polymer disk is indeed exposed outwardly facing the aqueous phase (Figure 1b). Similarly, after the paraffin wax is dissolved, the corresponding ball-on-disk asymmetric particles are obtained (Figure 1c). Size of the asymmetric PS particles is about 2−3 μm in diameter.

Let us further control the final morphology of the asymmetric polymer particles (Figure 2a). Two key variables, surfactant SDS concentration and cross-linking degree, are of main concern. At a fixed cross-linking degree (8.3 wt % DVB), no edge forms but a flattened side at very high level of SDS concentration (5 mg/mL) is observed, achieving a semispherical shape about 3 μm in diameter. With decrease in SDS concentration (2 mg/mL), the edge appears

dx.doi.org/10.1021/ma102945t |*Macromolecules* 2011, 44, 3787–3794

while the ball diameter shrinks to about 2 μm. At a very low level of SDS concentration (1 mg/mL), the edge becomes fully grown to be a disk while the ball diameter becomes smaller by about 1 μm. Besides SDS concentration, cross-linking degree is another key variable to control the shape of the particles. In the absence of DVB, no edge forms regardless of the SDS concentration. With increase in SDS concentration, curvature of the resulting particles is increased, and the shape transforms from flattened disk to spherical. When some amount of DVB is introduced (8.3 wt %), the edge appears again, which becomes larger with DVB content. On the basis of the experimental morphological evolution, it is convincible that the cross-linking degree is the key factor to determine the ball-on-disk structure. At higher cross-linking degree, swelling of polymer particles with the monomers becomes more difficult, which is conducive to enrichment of the residual monomers at the triple phase contact line. By polymerization of the monomers, an edge forms and becomes fully grown at higher DVB content. In addition, higher SDS concentration above the cmc (cmc_{SDS} = 2.48 mg/mL, at 40 °C) will result in new monomer/SDS micelles. By polymerization, secondary free smaller spherical particles form (Figure S1, Supporting Information). Because of the competing effect, the amount of monomers forming the edge is decreased and the edge size becomes smaller. In order to avoid secondary polymer particles, the surfactant SDS should remain at low concentration level below the cmc. Recalling the contribution of cross-linking degree to the edge formation, a higher DVB content can also result in the formation of edge even at higher SDS concentrations.

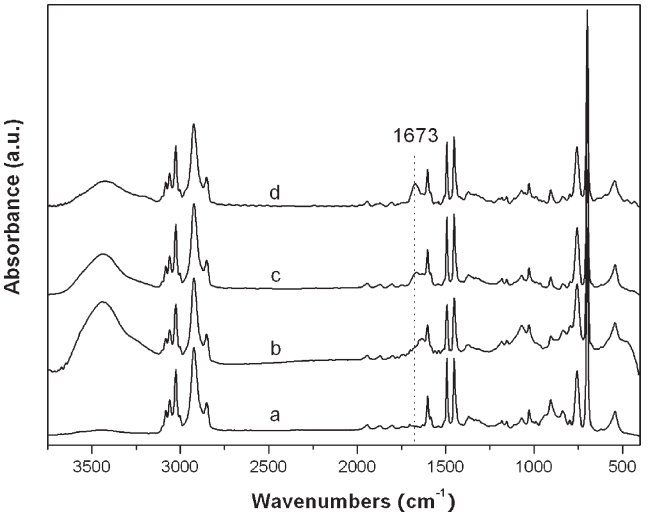

Figure 6. FT-IR spectra of some representative particles (shown in Figure 5) synthesized at increasing AM contents (*g*): (a) 0; (b) 0.2; (c) 1.0; (d) 2.0. The peak at 1673 cm^{-1} assigned to the C═O group of PAM.

During formation of the asymmetric shape, interfacial tension difference also plays roles in facilitating the flattening process dynamically and edge formation as shown in Figure 2b. Polymer becomes insoluble in paraffin wax and aggregate into a ball during polymerization. Because of the Pickering effect, the polymer ball tends to migrate at the O/W interface. Deformation of the polymer balls at the O/W interface can be explained according to elongation of those colloids at two-dimensional planar interface.[21] At the triple phase contact line, the difference among three interfacial tensions is responsible for the elongation, e.g. γ_{pw} (particle/water), γ_{po} (particle/oil), and γ_{ow} (oil/water). When SDS is absorbed at the exterior side of the ball exposed to the aqueous phase, a temporal Janus structure forms. As the exposed side of the polymer ball has been elongated, γ_{ow} should dominate over γ_{pw} plus γ_{po}. While an edge appears, the vector γ_{po} coincides with γ_{ow}. As result, the interfacial tension mismatch becomes weakening. The elongation terminates until three vectors reach equilibrium. According to interfacial tension measurement and calculation (Table 1), the increase of γ_{ow} with the decrease in SDS concentration is larger

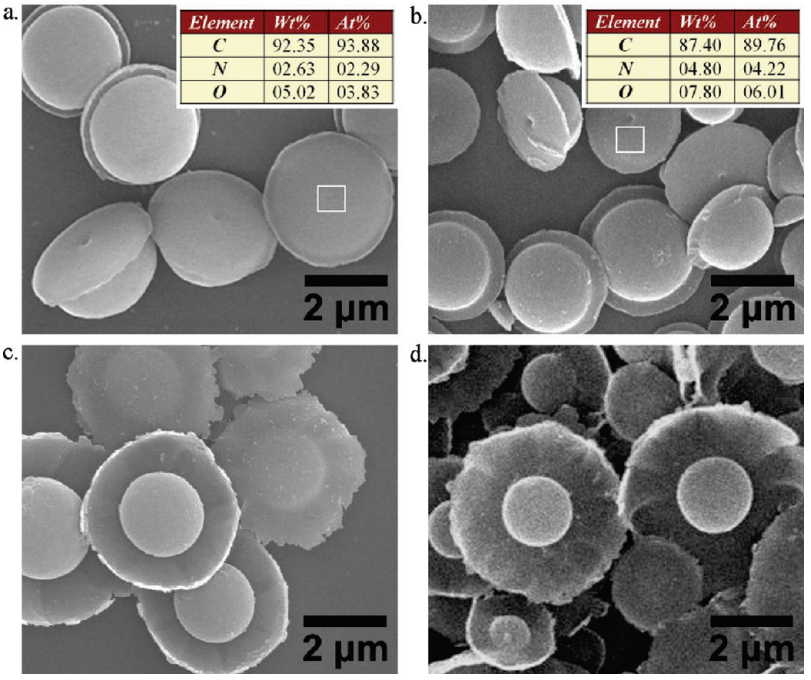

Figure 7. SEM images of some representative asymmetric Janus polymer particles synthesized when AM was added at the stages after different polymerization time (h): (a) 4; (b) 2; (c) 1; (d) 0.25. The inset EDX data corresponding to the frame area of the exposed side. AM content was fixed at 1 g and the SDS concentration was at 2 mg/mL.

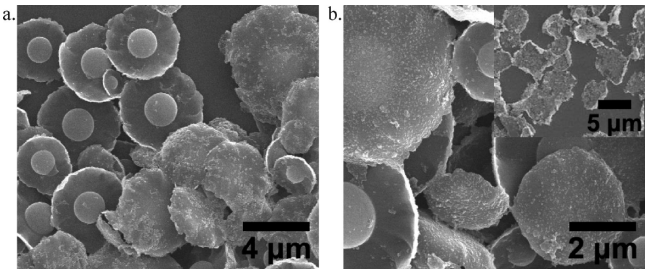

Figure 8. Two representative asymmetric Janus composite particles: (a) PS/PAM with Fe_3O_4 nanoparticles preferentially labeled onto PAM side; (b) PS/PAM/SiO_2 and the derived SiO_2 flakes by calcination of the polymer (inset SEM image).

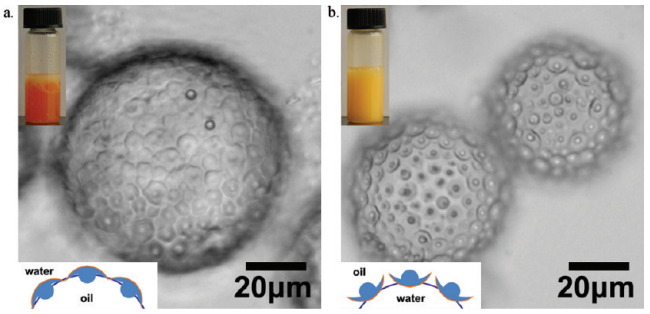

Figure 9. Two emulsions stabilized with the asymmetric Janus PS/PAM particles: (a) oil (styrene)/water (1:5) and (b) water/oil (*n*-heptane) (1:5). The PS/PAM Janus particle content was 0.2 wt %. Methyl orange was added to water as a chromogenic agent.

than that of γ_{pw}, which is conducive to further elongation of the exposed side with the decrease in SDS concentration. On the other hand, an excess elastic internal stress is restored due to overswelling of the cross-linked polymer network during growth of the polymer ball. The interfacial tension mismatch drives elongation, facilitating release of the stress and accelerating formation of the edge. The polymer ball is more easily elongated forming remarkable edge at lower monomer fraction in the oil phase, while the ball diameter is smaller (Figure 3). When the monomer fraction increases from 37.5 wt % to 54.5 wt %, semispherical balls form without edge. At lower fraction of 23.1 wt %, the ball becomes smaller about 1.5 μm in diameter, and the edge becomes larger.

Although the asymmetric polymer particles have Janus performance due to absorption of SDS onto their exterior side, the Janus characteristic is temporal which will become weakening upon progressive dissolution SDS from the ball (Figure 4a). Finally, SDS can be dissolved completely (Figure 4b). In order to introduce permanent Janus performance, an example hydrophilic PAM brush is polymerized onto the exposed side in the aqueous phase using the residual free radicals at the particles. The disk part becomes larger with increasing AM content while the ball part shrinks (Figure 5). The presence of PAM is confirmed by the characteristic band at 1673 cm^{-1} (assigned to the C═O group of PAM) (Figure 6), whose intensity increases with AM content (curves b−d). On the disk side, content of N element is high 12.68 wt % measured by energy dispersive X-ray (EDX), while no N element is detected on the ball side (Figure 5e). This confirms that PAM exclusively locates on the disk side, and the two compositions are distinctly compartmentalized onto both sides. Besides changing AM content, shape of the PAM terminated side is also tunable by AM addition time. For the polymer ball with one flattened side, when AM is added at very late stage of the ball formation after 4 h polymerization, there is a small edge although PAM brush forms onto the exposed flattened side. At an intermediate stage after 2 h polymerization, addition of AM gives the edge and N element content increases (Figure 7a,b). Accordingly, at very early stage after 1 or 0.25 h polymerization, addition of AM gives a remarkable disk (Figure 7c,d). This may be related with an easy release of the restored elastic stress of the polymer ball at early stage of polymerization. Since the surface area ratio between the hydrophilic PAM and the hydrophobic PS sides can be broadly adjusted, Janus balance of the particles can be controlled thereof.[22] Chemistry of both sides of the asymmetric PS/PAM Janus particles is further revealed by selective growth of materials on the desired sides. Citric acid capped Fe_3O_4 nanoparticles are preferentially adsorbed onto the disk side due to electrostatic interaction, while no nanoparticles are observed onto the ball side (Figure 8a). This also indicates that PAM is present exclusively onto the disk side. The corresponding paramagnetic composite Janus particles are achieved thereby. As another example, a sol−gel process of TEOS forming silica mainly occurs onto the PAM disk side (Figure 8b). After calcination in air at 450 °C for 2 h, the corresponding silica flakes are obtained (inset Figure 8b), revealing silica forms only onto the disk side. By further modification of the two sides and favorable growth of other materials therein, composition and microstructure of the particles will be extended deriving a huge family of asymmetric Janus composite particles.[15,20]

Since the Janus particles are amphiphilic, they should locate at the interface at a well-defined orientation. Meanwhile, oil/water immiscible mixture can be emulsified with the as-prepared PS/PAM Janus particles as solid surfactants. At 0.20 wt % of the PS/PAM Janus particles (as shown in Figure 5c), an oil (styrene)-in-water (O/W) emulsion forms at room temperature when oil is a minor phase (Figure 9a). Under optical microscope, it is clearly distinguished that the hydrophilic PAM disk part is exposed outwardly facing the external aqueous phase. This indicates that the asymmetric Janus particles have a well-defined orientation at the interface, which is essentially different from the homogeneous colloids rotating at the Pickering emulsion interface.[15] When oil becomes a major phase, a water-in-oil (W/O) emulsion forms (Figure 9b). The oleophilic PS ball part faces the external oil phase accordingly. When the paramagnetic Janus composite particles are used as a functional solid emulsifier, the dispersed droplets can be manipulated under a magnetic field.

4. CONCLUSION

In conclusion, we have reported a simple method to synthesize asymmetric Janus polymer particles at an emulsion interface. The polymer particles forms in situ in the internal oil phase by phase separation during emulsion polymerization, and immigrate toward the interface and anchor there due to Pickering effect. Morphological evolution of the particles with polymerization and their dependence on some key variables reveal that both cross-linking degree of the particles and interfacial tension difference play key roles in achieving the asymmetric shapes. By selective growth of functional materials onto the desired sides, composition and microstructure of the Janus particles can be controlled. The representative PS/PAM Janus particles are amphiphilic and can be used as solid surfactants to stabilize emulsions, which preferentially orientate at the interface. The method is general and scalable to derive a huge family of asymmetric Janus

composite particles, which is important to explore their practical applications.

■ ASSOCIATED CONTENT

Supporting Information. SEM image of the asymmetric polymer particles. This material is available free of charge via the Internet at http://pubs.acs.org.

■ AUTHOR INFORMATION

Corresponding Author

*E-mail: (C.Z.) zhangcl@iccas.ac.cn; (Z.Y.) yangzz@iccas.ac.cn.

■ ACKNOWLEDGMENT

We thank the NSF of China (Grants 50733004, 20720102041, and 50973121), Chinese Academy of Sciences (Grants KGCX2-YW-236 and KJCX2-YW-H20) and The Ministry of Science and Technology (Grant 2011CB933700) for financial support.

■ REFERENCES

(1) (a) Casagrande, C.; Fabre, P.; Raphaël, E.; Veyssié, M. *Europhys. Lett.* **1989**, *9*, 251. (b) de Gennes, P. G. *Rev. Mod. Phys.* **1992**, *64*, 645.

(2) (a) Perro, A.; Reculusa, S.; Ravaine, S.; Bourgeat-Lami, E.; Duguet, E. *J. Mater. Chem.* **2005**, *15*, 3745. (b) Yang, S. M.; Kim, S. H.; Lim, J. M.; Yi, G. R. *J. Mater. Chem.* **2008**, *18*, 2177. (c) Walther, A.; Müller, A. H. E. *Soft Matter.* **2008**, *4*, 663. (d) Wurm, F.; Kilbinger, A. F. M. *Angew. Chem., Int. Ed.* **2009**, *48*, 8412. (e) Wang, C.; Xu, C.; Zeng, H.; Sun, S. *Adv. Mater.* **2009**, *21*, 3045. (f) Jiang, S.; Chen, Q.; Tripathy, M.; Luijten, E.; Schweizer, K. S.; Granick, S. *Adv. Mater.* **2010**, *22*, 1060.

(3) (a) Glotzer, S. C.; Solomon, M. J. *Nat. Mater.* **2007**, *6*, 557. (b) Glotzer, S. C. *Science* **2004**, *306*, 419. (c) Blaaderen, A. V. *Nature* **2006**, *439*, 545.

(4) (a) Binks, B. P.; Fletcher, P. D. I. *Langmuir* **2001**, *17*, 4708. (b) Nonomura, Y.; Komura, S.; Tsujii, K. *Langmuir* **2004**, *20*, 11821. (c) Kim, J. W.; Lee, D.; Shum, H. C.; Weitz, D. A. *Adv. Mater.* **2008**, *20*, 3239.

(5) Behrend, C. J.; Anker, J. N.; Kopelman, R. *Appl. Phys. Lett.* **2004**, *84*, 154.

(6) (a) Lattuada, M.; Hatton, T. A. *J. Am. Chem. Soc.* **2007**, *129*, 12878. (b) Berger, S.; Synytska, A.; Ionov, L.; Eichhorn, K. J.; Stamm, M. *Macromolecules* **2008**, *41*, 9669.

(7) Nisisako, T.; Torii, T.; Takahashi, T.; Takizawa, Y. *Adv. Mater.* **2006**, *18*, 1152.

(8) (a) Ozin, G. A.; Manners, I.; Bidoz, S. F.; Arsenault, A. *Adv. Mater.* **2005**, *17*, 3011. (b) Valadares, L. F.; Tao, Y. G.; Zacharia, N. S.; Kitaev, V.; Galembeck, F.; Kapral, R.; Ozin, G. A. *Small* **2010**, *6*, 565.

(9) (a) Paunov, V. N.; Cayre, O. J. *Adv. Mater.* **2004**, *16*, 788. (b) Love, J. C.; Gates, B. D.; Wolfe, D. B.; Paul, K. E.; Whitesides, G. M. *Nano Lett.* **2002**, *2*, 891. (c) Lu, Y.; Xiong, H.; Jiang, X.; Xia, Y.; Prentiss, M.; Whitesides, G. M. *J. Am. Chem. Soc.* **2003**, *125*, 12724. (d) Koo, H. Y.; Yi, D. K.; Yoo, S. J.; Kim, D. Y. *Adv. Mater.* **2004**, *16*, 274.

(10) (a) Reculusa, S.; Poncet-Legrand, C.; Perro, A.; Duguet, E.; Bourgeat-Lami, E.; Mingotaud, C.; Ravaine, S. *Chem. Mater.* **2005**, *17*, 3338. (b) Perro, A.; Reculusa, S.; Pereira, F.; Delville, M. H.; Mingotaud, C.; Duguet, E.; Bourgeat-Lami, E.; Ravaine, S. *Chem. Commun.* **2005**, 5542. (c) Yu, H.; Chen, M.; Rice, P. M.; Wang, S. X.; White, R. L.; Sun, S. *Nano Lett.* **2005**, *5*, 379. (d) Qiang, W.; Wang, Y.; He, P.; Xu, H.; Gu, H.; Shi, D. *Langmuir* **2008**, *24*, 606.

(11) (a) Erhardt, R.; Zhang, M.; Böker, A.; Zettl, H.; Abetz, C.; Frederik, P.; Krausch, G.; Abetz, V.; Müller, A. H. E. *J. Am. Chem. Soc.* **2003**, *125*, 3260. (b) Walther, A.; André, X.; Drechsler, M.; Abetz, V.; Müller, A. H. E. *J. Am. Chem. Soc.* **2007**, *129*, 6187. (c) Wurm, F.; König, H. M.; Hilf, S.; Kilbinger, A. F. M. *J. Am. Chem. Soc.* **2008**, *130*, 5876. (d) Nie, L.; Liu, S.; Shen, W.; Chen, D.; Jiang, M. *Angew. Chem., Int. Ed.* **2007**, *46*, 6321.

(12) (a) Nie, Z.; Li, W.; Seo, M.; Xu, S.; Kumacheva, E. *J. Am. Chem. Soc.* **2006**, *128*, 9408. (b) Shepherd, R. F.; Conrad, J. C.; Rhodes, S. K.; Link, D. R.; Marquez, M.; Weitz, D. A.; Lewis, J. A. *Langmuir* **2006**, *22*, 8618. (c) Dendukuri, D.; Pregibon, D. C.; Collins, J.; Hatton, T. A.; Doyle, P. S. *Nat. Mater.* **2006**, *5*, 365. (d) Nisisako, T.; Torii, T. *Adv. Mater.* **2007**, *19*, 1489.

(13) (a) Yin, Y.; Lu, Y.; Gates, B.; Xia, Y. *J. Am. Chem. Soc.* **2001**, *123*, 8718. (b) Xia, Y.; Yin, Y.; Lu, Y.; McLellan, J. *Adv. Funct. Mater.* **2003**, *13*, 907.

(14) Roh, K. H.; Martin, D. C.; Lahann, J. *Nat. Mater.* **2005**, *4*, 759.

(15) (a) Kim, J. W.; Larsen, R. J.; Weitz, D. A. *J. Am. Chem. Soc.* **2006**, *128*, 14374. (b) Zhang, C. L.; Liu, B.; Tang, C.; Liu, J. G.; Qu, X. Z.; Li, J. L.; Yang, Z. Z. *Chem. Commun.* **2010**, 4610. (c) Tang, C.; Zhang, C. L.; Liu, J. G.; Qu, X. Z.; Li, J. L.; Yang, Z. Z. *Macromolecules* **2010**, *43*, 5114.

(16) (a) Pickering, S. U. *J. Chem. Soc. Trans.* **1907**, *91*, 2001. (b) Aveyard, R.; Binks, B. P.; Clint, J. H. *Adv. Colloid Interface Sci.* **2003**, *100*, 503. (c) Hong, L.; Jiang, S.; Granick, S. *Langmuir* **2006**, *22*, 9495. (d) Liu, B.; Wei, W.; Qu, X.; Yang, Z. *Angew. Chem., Int. Ed.* **2008**, *47*, 3973. (e) Liu, B.; Zhang, C. L.; Liu, J. G.; Qu, X. Z.; Yang, Z. Z. *Chem. Commun.* **2009**, 387.

(17) Zerrouki, D.; Baudry, J.; Pine, D.; Chaikin, P.; Bibette, J. *Nature* **2008**, *455*, 380.

(18) Dinsmore, A. D.; Hsu, M. F.; Nikolaides, M. G.; Marquez, M.; Bausch, A. R.; Weitz, D. A. *Science* **2002**, *298*, 1006.

(19) (a) Tanaka, T.; Okayama, M.; Kitayama, Y.; Kagawa, Y.; Okubo, M. *Langmuir* **2010**, *26*, 7843. (b) Ahmad, H.; Saito, N.; Kagawa, Y.; Okubo, M. *Langmuir* **2008**, *24*, 688.

(20) Wei, W.; Yang, Z. Z. *Adv. Mater.* **2008**, *20*, 2965.

(21) Park, B. J.; Furst, E. M. *Langmuir* **2010**, *26*, 10406.

(22) Jiang, S.; Granick, S. *Langmuir* **2008**, *24*, 2438.